IAC-24.A2.4.11

Experimental Analysis of Vibrationally–Induced Fluidization of Lunar Regolith in Hoppers and Closed Containers

Peter Watson[1], Sebastien Vincent Bonnieu[2], Ali Anwar[1,3], Marcello Lappa[1*]

[1]*Department of Mechanical and Aerospace Engineering, University of Strathclyde, James Weir Building, 75 Montrose Street, Glasgow, G1 1XJ, UK*
[2]*European Space agency, European Space Research and Technology Centre Keplerlaan 1 2201 AZ Noordwijk*
[3]*Weir Advanced Research Centre, 9 George Street, Glasgow, G1 1RD, UK*
[*]corresponding author email: marcello.lappa@strath.ac.uk

Abstract

In the coming years a major spotlight is being placed on our return to the Moon with the goal of further exploring and ultimately creating a permanent presence on our satellite. This naturally leads to the need to identify the best or most efficient way to exploit the "locally" available lunar resources. Along these lines, this study considers "vibrations" as a novel means to implement an efficient management and transport of the so-called "lunar regolith" abundantly available on the moon surface. Although such a line of inquiry can be placed in the larger theoretical context represented by the vibro-fluidization of granular materials, specific challenges emerge in this case due to the nature of the lunar regolith itself, which is typically characterized by strong frictional phenomena and ensuing electrostatic effects. Two partially intertwined problems are considered, one focusing on how the flow rate of lunar regolith simulant through the orifice of a hopper vessel of fixed inclination walls can be increased through the application of vibrations with various orientations, frequency and amplitude and a second scenario in which the samples are forced to enter a fluidized (convective) state inside a closed rectangular container. In the latter case a parametric investigation is also conducted to assess the role played by the particle size distribution (by using different types of simulants and/or simulants that have been sieved). The degree of achieved fluidization inside the closed container is determined by looking at the patterning behavior of the free surface of the material (where valleys and peaks tend to be created) and the convective motion itself established in its bulk. It is shown that regardless of the metrics used to quantitatively substantiate the level of fluidization and the considered system (closed or open), a similar non-monotonic relationship exists between this measure of fluidization and the frequency of the applied vibrations. An additional degree of complexity is brought about by the completely different effect that vibrations can have on the dynamics according to their relative orientation with respect to the direction of gravity.

Keywords: lunar regolith, fluidization, vibrations

Nomenclature

This section is not numbered. A nomenclature section could be provided when there are mathematical symbols in your paper. Superscripts and subscripts must be listed separately. Nomenclature definitions should not appear again in the text.

Acronyms/Abbreviations

1. Introduction

In the context of space exploration and colonization, especially regarding the Moon, the so-called "lunar regolith" presents both a challenge and an opportunity [1]. As humanity ventures farther into space and sets sights on establishing a sustainable human presence beyond Earth, the Moon is a natural first step.

One of the key resources available on the lunar surface is the regolith, a fine layer of dust and broken rock fragments that constitutes the Moon's surface. Understanding how to efficiently work with and utilize this material is critical, and one promising approach is finding ways to "fluidize" it using vibrations [2,3,4]. This process could be essential for a variety of reasons, including construction, resource extraction, and habitat development.

Lunar regolith differs significantly from the soils found on Earth. Unlike terrestrial soil, which is shaped by weathering and biological processes, lunar regolith is formed almost entirely through impact processes [5]. The constant bombardment of meteoroids has pulverized the surface rock, creating a fine, powdery substance that is sharp and angular, with no atmosphere or water to erode its edges. This makes the material

extremely abrasive and adhesive in both vacuum and gaseous environments, posing considerable challenges for mechanical equipment and infrastructure development. Additionally, lunar gravity is only about one-sixth of Earth's, which influences how materials behave when displaced or manipulated [5].

The idea of fluidizing the lunar regolith involves using mechanical vibrations to reduce its resistance to flow, effectively turning the dust and rock fragments into a more malleable or “fluid-like” substance that can be easily transported or shaped. This not a completely new idea or concept. Vibrations are widely recognized for their capacity to greatly mitigate the internal friction of various granular materials, thereby weakening their shear strength. Additionally, they influence the apparent rheology of the granular material by suppressing the yield stress [6,7].

On Earth, similar techniques are used in industries like construction and mining to transport granular materials [8,9], however adapting this concept for use with the lunar regolith requires an understanding of how this unique substance behaves when “shaken”. Most of the existing literature appearing over the last 30 years for vibrated granular matter has been produced assuming spherical particles and often “monodisperse” distributions, i.e. particles all having the same size [10], with scarce translational relevance to the aforementioned unique properties of lunar regolith.

Fluidizing lunar regolith could be crucial in several key areas of space exploration. One of the most immediate applications is in excavation and construction [11]. In order to build lunar bases or infrastructure on the Moon, we will need to relocate large amounts of regolith to clear areas, lay foundations, or create barriers for radiation shielding. Along the same lines, lunar regolith is nowadays regarded as a valuable resource for various branches of the ISRU (in-situ resource utilization) tree. As an example, regolith can be processed to extract oxygen and metals [12], and other useful elements, or it can be used in its raw form to produce bricks [13] or various types of concrete [14,15] or even as a substrate for plant growth [16].

Especially oxygen is abundant in the minerals that make up the regolith. To extract this element, the regolith must be heated to very high temperatures, which requires efficient handling and processing of large volumes of material. Vibrations could be used to fluidize the regolith, making it easier to move through processing equipment or into reactors for extraction. Furthermore, as outlined above regolith contains other valuable elements like silicon, aluminum, iron, magnesium, calcium, and titanium, which could be exploited to manufacture tools, equipment, solar panels and other necessities for lunar colonization.

However, the challenges associated with these objectives are considerable. As explained before, regolith’s unique properties—abrasiveness, abundance of cohesion, and electrostatic behavior—pose significant problems. Regolith particles can damage equipment by wearing down moving parts or jamming mechanisms, and their tendency to cling to surfaces in a vacuum environment complicates attempts to clean or remove them.

In this context, the ability to fluidize regolith would be critical in developing automated mining operations and processing facilities, and, remarkably, this concept applies to both “closed” and “open” systems. Whether contained within an enclosure, such as a sealed container, or exposed to the lunar or a gaseous environment in an open system, like a hopper or conveyor, understanding how to manipulate and control its movement is essential for various operations.

Closed systems, such as storage containers or reactors will often be used in the general context ISRU strategies for oxygen extraction or in holding large amounts of regolith to be used later as a feedstock for 3D printing [17] or for other construction or processing activities. In these cases, fluidizing the material via vibrations could ensure that it flows smoothly and does not become compacted or difficult to manipulate. Due to the low gravity and lack of atmosphere, regolith inside closed systems can settle unpredictably, potentially clogging equipment or settling in irregular patterns that complicate extraction processes. Vibrations could help redistribute the material evenly and prevent blockages, ensuring that the regolith can freely be directed towards tubes, valves, or other narrow spaces.

On the other hand, open systems like hoppers, pipes, or large-scale excavation equipment also face issues requiring attention [18] such as “jamming” or “arching”. Through numerous terrestrial experiments, it has been consistently observed that when the opening through which granular materials flow is too small, the flow comes to a stop. This phenomenon could be viewed as a kind of phase shift from liquid to solid. What sets it apart, however, is that it is governed entirely by mechanical stresses, with no influence from electrostatic forces. As the material accumulates within an open system like a hopper, the weight from the material above applies pressure to the lower layers. This growing pressure alters how the particles pack together, eventually leading to the formation of a "stable arch" or a self-supporting chain of particles. These arches can completely stop the flow of material, which is why the terms "jamming" and "arching" are often used interchangeably. Vibrations, when properly controlled, could assist in maintaining a steady flow of regolith through such open systems, preventing clumping, jamming and/or uneven distribution of material. This would be vital for automated mining operations, where continuous regolith movement is crucial to transport material from excavation sites to processing plants.

Additionally, it is also worth pointing out that controlling dust is a significant problem in open systems because lunar dust is both electrostatically charged and incredibly fine, allowing it to stick to equipment, clog filters, or interfere with machinery. Vibrationally-driven fluidization could mitigate dust accumulation by keeping particles in motion or dislodging them from critical surfaces before they can cause damage.

2. Material and methods

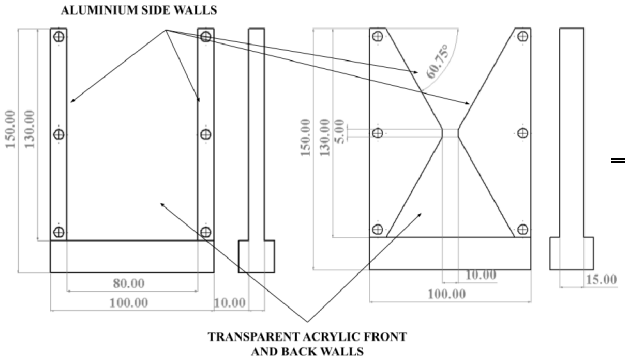

Figure 1. Sketch of the rectangular convection study vessel (left) and hopper vessel (right).

The geometry of the two different vessels employed in the experiments is presented in figure 1 with the rectangular vessel used for the particle size distribution (PSD) experiments on the left of the figure and the hopper vessel used for the flow rate experiments on the right. The side walls of both devices are made from aluminum while the front and back surfaces are made from transparent acrylic PVC to allow direct visualization of the dynamics of interest. In the hopper case an acrylic stopper is used to block the orifice to allow material to be added to the upper half of the hourglass (its removal causes the initiation of flow from the top to the bottom half of the hourglass).

The devices are bolted to the armature of a TIRA TV 51140 Vibration Test System via an aluminum mounting plate, which allows vibration in the range of 2 – 6500Hz and a peak force of 400N to be applied to the mounted device in the vertical direction. This vibration system is coupled with a Dytran 7503D4 triaxial accelerometer to allow the measurement of the acceleration amplitude (gamma) of the vibration signal applied during testing.

The materials used during these experiments were samples of the lunar regolith simulant material LHS-1 [19] produced by Exolith Lab. This is a material designed to mimic the physical and mechanical characteristics of the real lunar regolith, thus providing a reasonably accurate representation of the dynamics of interest. The properties of LHS-1 are summarized in Table 1.

Table 1. Key parameters of LHS-1 acquired from Exolith Labs: Geotechnical Properties

Uncompressed bulk density	2.75 g/cm^3
Mean particle size	90 μm
Median particle size	60 μm
Particle size range	< 0.04 - 1000 μm
Max angle of repose	47.5°
Cohesion	0.311 kPa
Angle of internal friction	31.49°

For the first type of experiments (Fig.1, left panel), the initial sample of LHS-1 with a PSD of 0.04µm-1000µm was sieved using #60 and #250 sieves to produce samples with <0.04µm - 250µm and <0.04µm - 90µm respectively. One other PSD sample of <0.04µm - 35µm was also used, but this sample was also purchased from the manufacturer, coming already in this size range, under the designation LHS-1D.
Layer heights of 30mm of each sample were added to the rectangular 2D cell, with care to level the top of the layer without compacting the material, then subjected to different combinations of frequency and amplitude of vibration to assess the materials convective response. The degree of the fluidization of the bed at each combination of vibrational parameters was then characterized by measuring the distance between the peak and valley of the generated convectional heap.

For the second type of experiments concerning the hopper device (Fig.1, right panel), the original unaltered LHS-1 sample was added in fixed quantities in terms of mass,25 and 45 grams, to the hopper vessel with the stopper in place to block the orifice. Vibrations of differing combinations of frequency and amplitude were then applied to the vessel, and the stopper was removed so to initiate the flow of material from the top to the bottom region. The material behavior for each vibration intensity was recorded by using a camera in order to determine the mass flow rate “a posteriori” as the ratio of the initial amount of material inserted into the hopper and the overall time needed to leave the upper region. For each test, the flow rate was averaged over ten measurements in order to obtain meaningful values from a statistical standpoint.

3. Theory and calculation

To quantify the vibration intensity applied during the experiments the following formula for the

nondimensional acceleration amplitude is employed in this study.

$$\Gamma = \frac{b\omega^2}{g} \quad (1)$$

Where b refers to the amplitude of the vibration, ω^2 is the square of the angular velocity and g is the gravity acceleration.

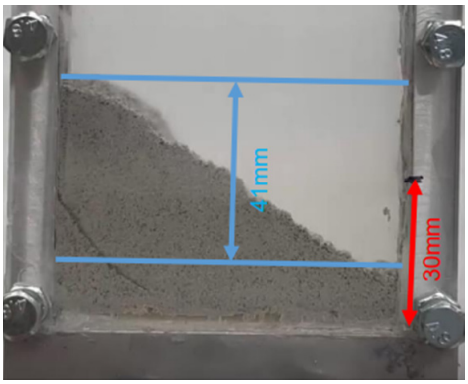

Figure 2. Degree of fluidization characterization from calculation of peak valley difference (mm)

Figure 2 shows the approach used to characterize the degree of fluidization of the convection heap formed from the PSD experiments in the closed cavity case. The reference length marked on the vessel, shown in red (denoting thirty millimeters from the vessel bottom to the desired height of the initial heap), is used to measure the peak valley difference.

As outlined before, to measure the mass flow rate of the lunar regolith simulant through the hopper orifice the mass of material in the hopper in its initial state is divided by time taken for the bed of material to fully flow through the orifice shown in Eq.(2).

$$\dot{m}_{LRS} = \frac{m_{LRS}}{t_f - t_i} \quad (2)$$

4. Results

The typical response of the tested beds of lunar regolith simulant to vibrations in the case of the closed cavity can be seen in Fig. 3, where a convection driven heap is clearly visible. In particular, Fig 3(a) shows the bed prior to vibration and Fig 3(b) reveals the generation of surface instabilities, which eventually progress into the formation of a large heap (Fig. 3d). The heap is driven by material flowing down the heap's surface, which after reaching its bottom, is driven inward and eventually up back to the top of the heap, thereby creating a self-sustaining planar (transverse) loop. This convective regime is typical for all particle size distributions investigated and allows for the quantification of the degree of fluidization in the bed as explained before.

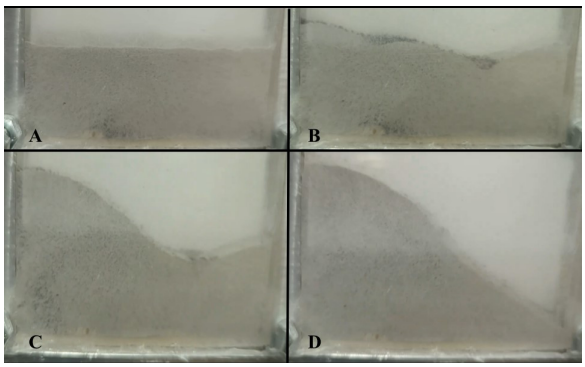

Figure 3. Images of convective flow regime during vibration for a) initial bed prior to vibration, b) – d) subsequent stages culminating in convective heap formation (f = 50 Hz, Γ = 5)

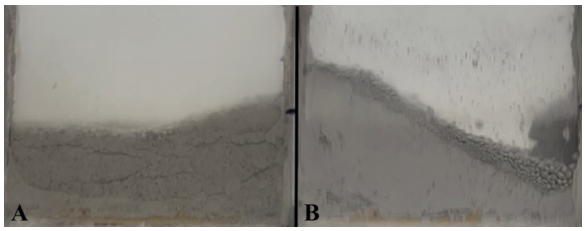

Figure. 4. Interesting additional convective responses during vibration a) longitudinal convection (f = 45 Hz, Γ = 5), b) particle accumulation at decreased PSD (<0.04μm - 35μm) (f = 45 Hz, Γ = 5)

Additional insights into the dynamics of the simulant in closed system case can be gathered from Fig. 4, where two convective regimes diverging from the normal mode previously described can be spotted. In particular, Fig 4(a) presents a case where the direction of the convection roll is perpendicular to the page (longitudinal roll). This was found only to occur in a small range of frequencies (close to 50Hz) but to exist for all values of increasing acceleration (Γ = 1 – 5). Fig 4 (b) shows a case with particles accumulating into large spherical clumps on the surface of the convective heap. This effect was observed for a small range of frequencies of around 35 – 50Hz, all values of investigated vibration intensity (Γ = 1 – 5) and when using the material with size distribution 0.04μm - 35μm. Although a proper interpretation of it would require additional investigation, some evidence has been found that it was likely due to the increased prevalence of electrostatic effects within this size range.

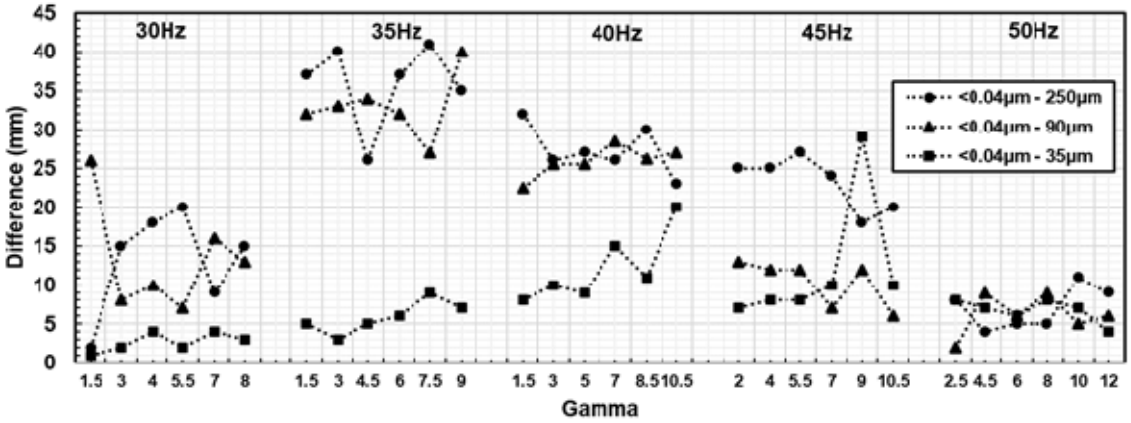

Figure 5. Degree of fluidization characterization for three different PSD, <0.04μm - 250μm, <0.04μm - 90μm and <0.04μm - 35μm

Figure 5 depicts the degree of fluidization (peak valley difference) as a function of the intensity and frequency of the applied vibration in the closed system (cavity) case.

The aforementioned peak-to-valley difference is shown over the frequency range 30-50Hz in order of increasing vibration intensity Γ for the 3 different PSDs previously described (denoted by 3 different symbols, the reader being referred to the Figure legend).

By visual inspection of this figure, the reader will realize that the peak-to-valley difference varies non-monotonically as the vibration intensity is increased and the effective dependence changes according to the considered specific frequency. Another interesting observation concerns the effect of decreasing the PSD (making the average particle size progressively smaller). Remarkably, for each frequency other than 50 hertz, the general trend appears to be that decreasing the PSD affects in a detrimental way the degree of fluidization. The behavior for the 50 hertz is different as the degree of fluidization for each of the PSD appears to be relatively the same in comparison with the other cases.

The typical flow regime for the hopper configuration without vibration is presented by figure 6, with progression from the initial unperturbed bed in Fig 6(a) to the fully discharged hopper in Fig 6(d). Fig 6(b) shows the effect on the held material after the hopper orifice is opened, with the tendency of the bed to collapse first in the middle being very evident. Interestingly, as witnessed by this figure, the two portions of the bed in contact with the hopper walls rigidly hold their position for a relatively long time. Only upon the middle of the bed fully discharging, these sections begin to move and one side collapses into the middle section.

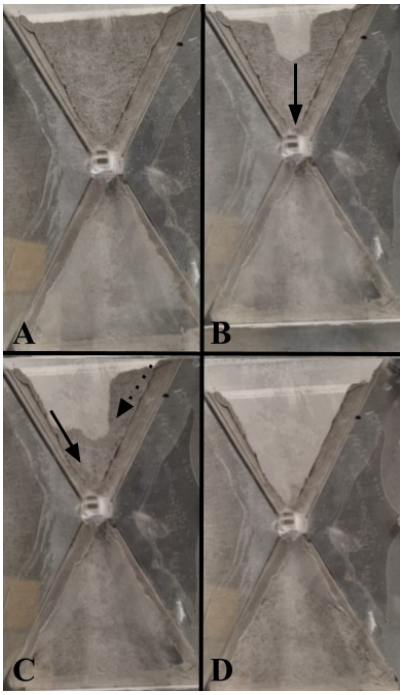

Figure. 6. Images of hopper discharging without vibrations a) initial bed prior to orifice opening, b) - d) subsequent stages of hopper discharging

This is very evident in Fig 6(c), where upon the falling sections full discharge through the orifice, the final remaining side wall section also collapses into the middle of the vessel and flows through the orifice. These findings clearly indicate that initial motion of the middle section of the beds through the orifice plays a crucial role in the overall dynamics when no vibrations are applied.

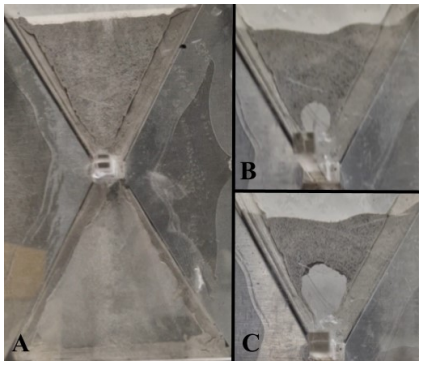

Figure 7. Hopper flow restricting mechanisms a) no flow, b) small arch and c) large arch

The major importance of the next figure of this sequence (Fig. 7) resides in its ability to show that for this material, occasionally an "arch" may form like those visible in Figs 7(b) 7(c). This arch may be regarded as a "stable" structure preventing the bed above from flowing down. We have observed this phenomenon to be dominant in all cases where vibrations were not applied.

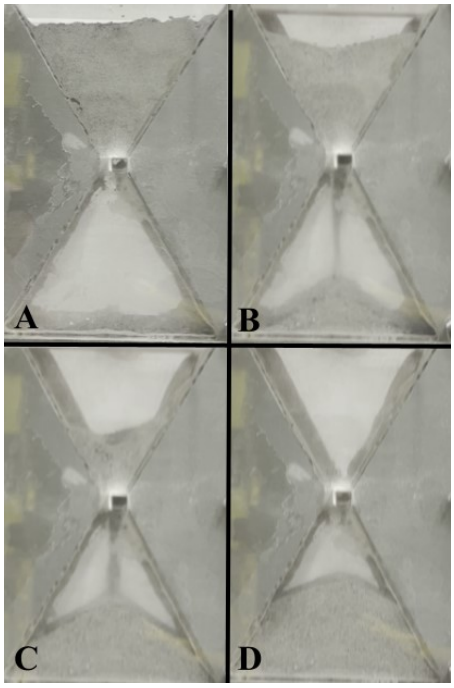

Figure 8. Images of hopper discharging under vibration a) initial bed, b) - d) subsequent stages of hopper discharging under vibration (f = 30 Hz, Γ = 2)

What stands immediately out from Fig. 8 is that the typical hopper flow regime during shaking is noticeably different, as it displays a substantially more ordered and symmetrical evolution. In particular, a first key observation stemming from Fig. 8 (b) is the U-shaped surface of the vibrated bed as the material flows through the orifice. This indicates that the bed flows uniformly downward with the greatest flow in the middle of the bed being comparable to that experienced by the side sections.

A second key observation concerns the intensity of the flow. Notably, while more ordered, the flow tends to be substantially slower than the case of no vibration, which may be regarded as a drawback. Nevertheless, no arching phenomena have been detected in such cases.

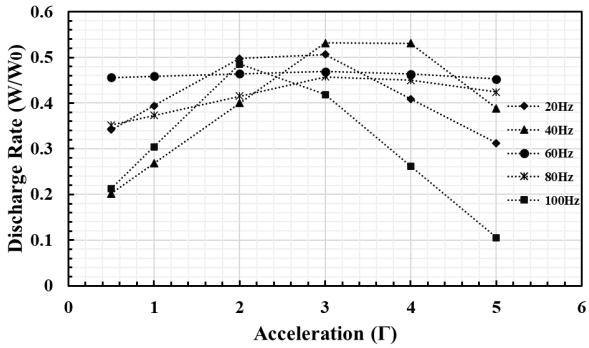

Figure 9. Hopper discharge rate as a function of acceleration and frequency

Figure 8 is complemented by Fig. 9, which provides quantitative information about the discharge rates (W/Wo) effectively obtained over the considered range of vibration frequency and amplitude (where Wo denotes the reference case without vibration). This figure is instrumental in demonstrating that a complex relationship exists between the flow rate and the acceleration amplitude (Γ) for each frequency as Γ is increased. The resulting discharge rate varies in a non-monotonic way with mid-range acceleration of around Γ = 2.5 maximizing the discharge rate and Γ = 0 and 5 yielding the opposite effect, i.e. a minimization of the ratio W/Wo.

The same complex relationship is further illustrated in Figure 10, where the three-dimensional colourmap quantitatively substantiates the variations of the discharge rate as a function of the frequency and acceleration of the applied vibrations.

This figure reveals that specific combinations of frequency and acceleration of vibration exist within the range 0 – 500Hz and Γ = 0 – 5 that maximize or minimize the mass flow rate of lunar regolith simulant through the hopper orifice. Due to the complex nature of the material investigated these results present an interesting finding in comparison to previously

investigated "monodisperse" beds of material, highlighting the need for further research in this field.

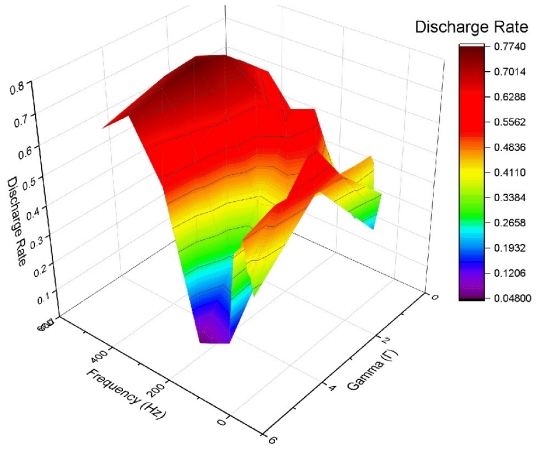

Figure 10. Hopper discharge rate as a function of acceleration and frequency 3D color map

Remarkably, from these finding it is evident that in none of the considered cases does the vibration increase the discharge rate over the no vibration case (the ratio W/Wo is always smaller than one), nevertheless, vibrations have a significantly beneficial effect, that is, they consistently permit the initiation of flow by preventing the lunar regolith simulant from forming arches.

Moreover, interestingly, convective rolls, resembling those described previously for the closed cavity, are also formed in the hopper and exert a role on the overall dynamics by restricting the flow of material through the orifice, thereby permitting a more controlled and symmetrical discharge of material with respect to the no vibration case.

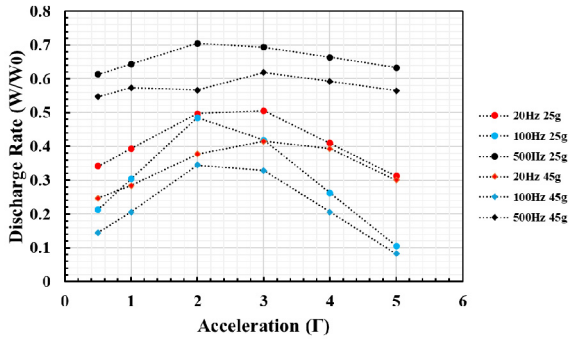

Figure 11. Effect of mass of hopper contents on the discharge rate as a function of acceleration and frequency

Figure 11 finally explores the role of another potentially influential parameter, namely, the initial mass of the bed of material placed in the hopper. With each color representing cases of the same frequency and different symbols exploited to identify different masses, this figure indicates that the discharge rate for the lesser mass is always greater than for the larger mass. This relationship was also found at all the intermediate frequencies in the frequency range.

This may be regarded as a logical finding if one considers that an increase in the initial mass of the bed should theoretically increase the compaction of the material under its own weight, thus strengthening the internal frictional effects. Along these lines, we would like to highlight that, as an example, we observed arching phenomena more frequently in the no vibration case, on increasing the initial mass.

5. Conclusions

These arguments make evident how vibrations can be used to fluidize the lunar regolith and foster accordingly the success of lunar operations. Whether in sealed reactors or open excavation systems, developing efficient methods for controlling the movement of lunar regolith is necessary to enable sustainable exploration, resource extraction, and habitat construction on the Moon. Effective solutions will streamline operations, reduce equipment wear, and ensure a more reliable infrastructure for long-term lunar habitation.

Most prominently the presented results describe similarly complex scenarios for both the open and closed considered systems, highlighting the significance of the problem and the need for additional analysis of the underlying dynamics to determine the most effective application of vibration for the desired purpose.

Acknowledgements

This work has been financially supported by the European Space Agency, ESA Contract 4000138607/22/NL/GLC/my, the Open Space Innovation Platform (OSIP). The authors wish to acknowledge also the support of EPSRC for contributing to the PhD scholarship of P. Watson.

References

[1] Rasera, J.N., Cilliers, J.J., Lamamy, J.A. and Hadler, K., 2020. The beneficiation of lunar regolith for space resource utilisation: A review. Planetary and Space Science, 186, p.104879.

[2] Lappa M., (2024), "New methods for the transport and management of lunar regolith", article in "Why Space? The Opportunity for Material Science and Innovation", a publication of UKRI-STFC and the Satellite Applications Catapult, ISBN: 9781914241680,

pp. 131-133 https://sa.catapult.org.uk/why-space-the-opportunity-for-material-science-and-innovation/
r-material-science-and-innovation/

[3] Watson P., Bonnieu S. V.and Lappa M., (2023), Effect of Vertical and Horizontal Vibrations, Vessel Size and Layer Height on the Fluidization of Lunar Regolith, Article ID: ICAMAE-2023-5-26 in Proceedings of First Joint International Conference on Advances in Mechanical & Aerospace Engineering (ATCON 2: ICAMAE 2023), November 28 - 30, 2023, Glasgow, UK – Book of Abstracts, ISBN: 978-81-965909-4-9, pp. 238-239.

[4] Watson P., Bonnieu S. V.and Lappa M., (2024a), Convective states and patterning behavior in Lunar Regolith under the effect of vertical vibrations, Book of Abstracts of the UK Fluids Conference 2023, 17-19th October 2023, Glasgow, UK - Editors M. Fossati, K. Kontis, M. Lappa, M. Oliveira, E. Chaparian, ISBN 978-1-914241-69-7.

[5] Walton O., (2012), "Challenges in Transporting, Handling and Processing Regolith in the Lunar Environment" in Moon: Prospective Energy and Material Resources, Viorel Badescu (Ed.), Springer, New York, 2012, pp. 267-294

[6] Roberts, A.W. and Scott O.J., (1978), An investigation into the effects of sinusoidal and random vibrations on the strength and flow properties of bulk solids. Powder Technol.21: 45–53

[7] Kollmann T., Tomas J., (2002), Effect of applied vibration on silo hopper design, Particul. Sci. Technol. 20 (1), 15–31.

[8] Suzuki A., Takahashi H., and Tanaka T., (1968), "Behavior of a particle bed in the field of vibration. II. Flow of particles through slits in the bottom of a vibrating vessel", Powder Technol., 2, 72-77.

[9] Zhang C., Qiu C., Pu C., Fan X. and Cao P., (2018), The mechanism of vibrations-aided gravitational flow with overhanging style in hopper, Powder technology, 327, 291-302.

[10] Watson P., Bonnieu S. V. and Lappa M., (2024b), "Fluidization and Transport of Vibrated Granular Matter: A Review of Landmark and Recent Contributions", Fluid Dynamics & Materials Processing, 20(1), 1-29. DOI: 10.32604/fdmp.2023.029280

[11] Zacny K., (2012), "Lunar Drilling, Excavation and Mining in Support of Science, Exploration, Construction, and In Situ Resource Utilization (ISRU)" in Moon: Prospective Energy and Material Resources, Viorel Badescu (Ed.), Springer, New York, 2012, pp. 235-266.

[12] Guerrero-Gonzalez, F.J. and Zabel, P., 2023. System analysis of an ISRU production plant: Extraction of metals and oxygen from lunar regolith. Acta Astronautica, 203, pp.187-201.

[13] Torre, R., Cowley, A. and Ferro, C.G., 2024. Low binder content bricks: a regolith-based solution for sustainable surface construction on the Moon. Discover Applied Sciences, 6(3), p.88.

[14] Ponnada, M.R. and Singuru, P., 2014. Advances in manufacture of Mooncrete–a Review. Int. J. Eng. Sci. Adv. Technol, 4(5), pp.501-510.

[15] Hu, Z., Shi, T., Cen, M., Wang, J., Zhao, X., Zeng, C., Zhou, Y., Fan, Y., Liu, Y. and Zhao, Z., 2022. Research progress on lunar and Martian concrete. Construction and Building Materials, 343, p.128117.

[16] Duri, L.G., Caporale, A.G., Rouphael, Y., Vingiani, S., Palladino, M., De Pascale, S. and Adamo, P., 2022. The potential for lunar and martian regolith simulants to sustain plant growth: a multidisciplinary overview. Frontiers in Astronomy and Space Sciences, 8, p.747821.

[17] Suhaizan, M.S., Tran, P., Exner, A. and Falzon, B.G., 2023. Regolith sintering and 3D printing for lunar construction: An extensive review on recent progress. Progress in Additive Manufacturing, pp.1-22.

[18] Reiss P., Hager P., Hoehn A., Rott M., Walter U., (2014), Flowability of lunar regolith simulants under reduced gravity and vacuum in hopper-based conveying devices, Journal of Terramechanics, 55, 61–72.

[19] Space resource tech, Lunar highlands simulant (LHS-1) high fedelity moon dust simulant, 07/31/2023,https://spaceresourcetech.com/products/lhs-1-lunar-highlands-simulant, accessed 28/09/24